EUROFUSION WPS1-CP(16) 15090

KJ McCarthy et al.

Plasma Core Fuelling by Cryogenic Pellet Injection in the TJ-II Stellarator

Preprint of Paper to be submitted for publication in
Proceedings of 26th IAEA Fusion Energy Conference

Plasma Core Fuelling by Cryogenic Pellet Injection in the TJ-II Stellarator

K. J. McCarthy[1], N. Panadero[1], J. L. Velasco[1], J. Hernández[1], S. Satake[2], D. López Bruna[1], R. García[1], J. Baldzuhn[3], A. Dinklage[3], E. Ascasibar[1], and TJ-II team[1]

[1]Laboratorio Nacional de Fusión, CIEMAT, Madrid, Spain

[2]National Institute for Fusion Science, Toki, Japan

[3]Max-Planck-Institut für Plasmaphysik, Greifswald, Germany

E-mail contact of main author: kieran.mccarthy@ciemat.es

Abstract. Core fuelling is a critical issue on the pathway to the development of steady-state scenarios in magnetically confined plasma devices, in particular, for helical devices. Indeed, neoclassical theory predicts that on-axis electron cyclotron resonance heating (ECRH) necessitates a particle source situated at the same radial position as ECRH with an analogous deposition profile shape in order to mitigate potential core particle depletion. A prime candidate for core fuelling is cryogenic pellet injection, a technology that has been employed for several decades. However, a detailed understanding of pellet ablation mechanisms, and subsequent particle transport, remains outstanding and is of paramount interest. Pellet injection studies on the stellarator TJ-II, with relevant parameter variations, can provide valuable input for, for instance, the W7-X pellet injection program, this being of critical importance for neoclassical transport optimization in W7-X and the attainment of long-pulse high-power discharges with pure microwave heating (the "standard" W7-X discharge scenario). Here, pellet experiments, performed using a compact pellet injector on TJ-II, are reported together with estimates of pellet penetration and fuelling efficiency for ECRH and/or neutral beam injection heated plasmas created using the standard TJ-II magnetic configuration.

1. Introduction

Plasma core fuelling is one of several important challenges for achieving steady state operation in magnetically confined fusion reactors [1, 2]. Although gas puffing is a well-established tool for sustaining plasmas in current fusion devices, its position outside the plasma edge means that this technique will be inefficient in large devices. Moreover, it is predicted that particle recycling will be minimal since plasma-wall interactions will predominantly occur close to, or in, the divertor region. On the other hand neutral beam injection (NBI) heating systems can also contributes to plasma core fuelling [3]. However, the introduction of such an energy source might be problematic from the point of view of density control, in particular in stellarator devices, in which energy and particle transport are coupled in the core [4]. Furthermore, in the case of heliac devices, such coupling is predicted to lead to hollow density profiles, and subsequent loss of plasma control, thereby reinforcing the need for fuelling techniques that circumvent such drawbacks [5]. Nonetheless, there exists a good and well-developed candidate, cryogenic pellet injection. It is a technology that has been used on magnetically confined plasma devices for several decades [6, 7] with the advantage of achieving relatively localized core fuelling without an associated energy source.

Cryogenic pellet injection has been, and continues to be, the subject of significant research in tokamaks and, in particular, in stellarators. For example, studies performed on the W7-AS stellarator provided good agreement between experimental and predicted penetration depths while also indicating some influence of central electron temperature, $T_e(0)$, on fuelling efficiency [8]. In the Large Helical Device (LHD), pellet injection has allowed extending the operational regime with good energy confinement [9, 10]. More recently, in the medium-sized stellarator TJ-II, several experimental and theoretical comparative studies have been performed recently using a newly installed pellet injector [11]. One such study has demonstrated for certain scenarios, that particle transport can redistribute some outlying pellet particles inwards towards the core, thereby slowing down core depletion [12]. Moreover, for the recently commissioned W7-X helias device, the commissioning of a pellet injector is a priority for studying plasmas with electron cyclotron resonance heating (ECRH). Finally, a preliminary comparative study of pellet ablation and confinement was made on the LHD and TJ-II devices has provided valuable input for this device [13].

In this report pellet fuelling studies performed on the stellarator TJ-II are reported. For this, cryogenic hydrogen pellets are injected from its low-field side into ECRH or NBI heated plasmas in order to pellet particle deposition and evolution about its magnetically confined plasma and to determine the ratio between pellet particles deposited in the plasma and pellet particle content over a range of target plasma densities. Finally, other pellet related issues, such as the influence of suprathermal electron populations on the ablation process, are also considered.

2. TJ-II Experimental set-up

The TJ-II, a low magnetic shear stellarator of the heliac type designed to have a high degree of magnetic configuration flexibility, has a major radius of 1.5 m and an average minor radius, r, of ≤ 0.22 m [14]. Its magnetic field at plasma centre, B(0), is ≤ 1.1 T. Plasmas, created using hydrogen, deuterium or helium as the working gas, are created and maintained using ECRH with one or two gyrotrons operated at 53.2 GHz, *i.e.*, the 2nd harmonic of the electron cyclotron resonance frequency ($P_{ECRH} \leq 500$ kW, $t_{discharge} \leq 300$ ms). Additional heating is available by the injection of accelerated neutral hydrogen atoms ($E_{NBI} \leq 32$ keV, $P_{NBI} \leq 1$ MW) from two tangential NBIs operating parallel and anti-parallel to the magnetic field direction. Note: here the term counter is employed for injection in the same direction as the magnetic field, *i.e.* parallel injection, and the term co-injection for injection in the opposite direction, *i.e.* anti-parallel injection [15]. With ECRH, central electron densities, $n_e(0)$, and temperatures, $T_e(0)$, up to 1.7×10^{19} m^{-3} and 1 keV, respectively, can be achieved. Additional heating by NBI heating results in plasmas with $n_e(0) \leq 5\times10^{19}$ m^{-3} and $T_e(0) \leq 400$ eV when a lithium coating is applied to the vacuum vessel wall [16]. Plasma discharges have also been created using Neutral Beam Injectors (NBI) only by injecting the counter beam into a seed plasma during the final stage of the magnetic field ramp-up.

2.1.TJ-II Pellet Injector

A compact pellet injector, developed in conjunction with the Fusion Energy Division of Oak Ridge National Laboratory, Tennessee, USA, operates on the TJ-II. It is equipped with a cryogenic refrigerator for *in-situ* hydrogen pellet formation, fast propellant valves for pellet acceleration (800 to 1200 m/s), in-line diagnostics for determining pellet velocity and mass [17], plus delivery lines. In total, up to 4 pellets, which are fabricated in-situ, can be injected per TJ-II discharge. Pellets with diameters 0.42 mm (*Type*-1) and 0.66 mm (*Type*-2) (containing 3×10^{18} and 6×10^{18} hydrogen atoms, respectively) are generally used for experiments in which the electron density cannot rise above the gyrotron cut-off limit (~1.7×10^{19} m^{-3}). Larger pellets, with diameters of 0.76 mm (*Type*-3) and 1 mm (*Type*-4) and containing $\leq1.8\times10^{19}$ and $\leq4.1\times10^{19}$ H particles, respectively, can be injected into higher density NBI-heated plasmas. Notes: for the standard TJ-II magnetic configuration the plasma volume contained within the last-closed magnetic surface (LCMS) is ~1.1 m^3 and pellets are injected from the low-field side of the device. Optical access to the full pellet path through the plasma is available through ports located above (TOP) and behind (SIDE) the pellet flight path. See Figure 1 of Ref. [11]. The light emitted by the neutral, or partially ionized, cloud surrounding an ablating pellet, is collected by amplified silicon diodes and used to create a pellet ablation emission profile along its flight path through the plasma [11].

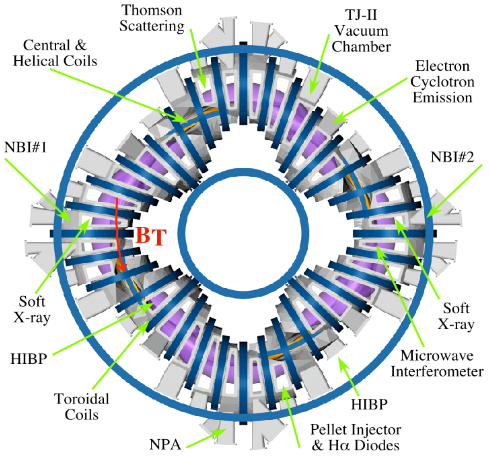

FIG. 1. Birds-eye view sketch of the TJ-II stellarator highlighting selected device systems and principal diagnostics.

2.2.Associated Plasma Diagnostics

The TJ-II is equipped with a wide range of plasma diagnostics [18], *e.g.* a Thomson Scattering (TS) system that provides one set of electron density and temperature profiles per discharge [19], a microwave interferometer that follows the line-integrated electron density evolution along a discharge. Note: the microwave interferometer has 10 μs temporal resolution. These systems are located at 180° and 67.5° toroidally, respectively, from the PI. See Figure 1. Other diagnostics of interest include an 11 channel Electron Cyclotron Emission (ECE) system to follow the electron temperature evolution at different radii, a multiple-filter soft X-ray diagnostics to follow the temporal evolution of the core electron temperature [20], broadband bolometer arrays, two heavy ion beam probe systems, Mirnov coil arrays to measure local magnetic field components, and neutral particle analyzers to obtain the ion temperature [18].

2.3.Experiments

In the experiments described here, pellets containing from 0.5 to 1.5×10^{19} hydrogen particles are injected into plasmas created using the standard magnetic configuration, 100_44_64, where the nomenclature reflects currents in the central, helical and vertical field coils, respectively. Note: hydrogen was also used here as the working gas. The initial pellet particle deposition across the plasma radius, and its subsequent radial evolution along a discharge, are determined using the shot-to-shot technique where pellets are injected into reproducible plasmas and single TS measurements are made at different times before, during and after pellet injection. In addition, the fuelling efficiency can be determined from the increase in plasma particle content after pellet injection. For this, plasma particle content is obtained by integrating the TS electron density profile over the whole plasma volume, assuming an average plasma minor radius of 0.1925 m for the 100_44_64 configuration. In parallel, the pellet particle content is obtained by assuming that pellet mass loss between the microwave cavity and plasma edge is negligible because of the relatively short length (~1.1 m) of the straight guide tubes. As a TS calibration check, the line-integrated density is estimated along the TS density profile for comparison with the measured line-averaged electron density. It should be noted that due to the design of the pellet injector and the plasma geometry, the flight path followed by pellets fired from lines 2 and 3 does not cross the plasma centre, rather for the nominal magnetic configuration, the closest approaches are ρ = 0.273 and 0.45, respectively [11]. However, this has been modified recently (for discharges after #41715) so that Type-2 pellets can now reach the plasma centre, ρ = 0, *e.g.*, for data in Figure 2.

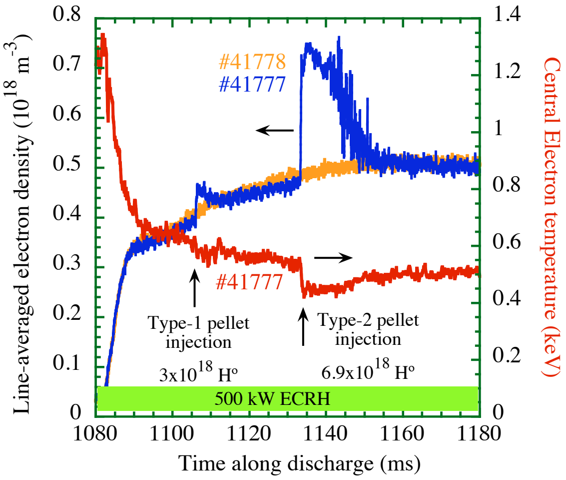

FIG. 2. Evolution of line-averaged electron density and central electron temperature along reproducible ECRH discharges with and without pellet injections.

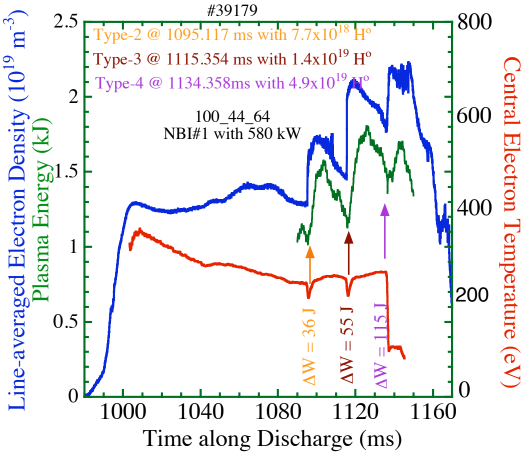

FIG 3. The temporal evolution of several plasma parameters during sequential pellet injections into a NBI plasma. Note: the 3rd pellet causes plasma collapse.

3. Results and Analysis

In a previous work it was outlined how a pellet ablation profile is obtained in the TJ-II from the recorded Balmer H_α spectral line (λ = 656.3 nm) light [11]. Similarly, it was shown how the electron temperature radial profile, as provided by the TS system, is strongly perturbed immediately by the inward travelling pellet when the passing pellet cools the local plasma immediately, this being followed by a slower radial cooling outwards. Subsequently, in NBI heated plasmas the T_e profile recovers to, or increases above, pre-injection values within a few milliseconds (Figure 3). In contrast, for ECRH-only plasmas, the ensuing T_e values remain significantly lower than pre-injection values during an extended period (Figure 2).

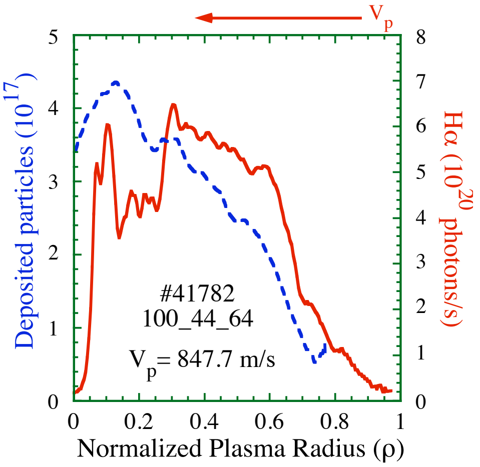

FIG 4. Pellet electron radial distribution 3.9 ms after injection (blue) and Hα signal (red) profile emitted during pellet ablation.

In parallel, the evolution of the electron density is significantly slower, requiring several milliseconds to achieve complete particle distribution about the plasma. In the first instances, the form of the initial pellet particle deposition across the plasma minor radius is well described by the Balmer H_α emission (see Figure 4). Note: in Figure 4, in which the plasma edge to plasma centre distance is 0.17 m, the pellet is fully ablated ~200 ms after entering the plasma. Also, in this same figure, no enhanced ablation due to impacts with suprathermal electrons is observed for this ECRH plasma. This holds for both on- and off- axis heating and for relevant all plasma target densities. Subsequently, after complete ablation, pellet particles continue to be distributed about the plasma. This intervening time encompasses ionization of the neutral gas cloud that surrounds the pellet and the subsequent diffusion of its particles around the plasma. See Figure 5, where a scan, made using shot-to-shot TS profiles obtained using reproducible ECRH plasmas, highlights this. From this a radially inward transport of pellet particles towards the core is perceived. Next, by integrating these profiles over the full plasma volume (and assuming a uniform toroidal distribution), the temporal evolution of the pellet particle population can be extracted. See Figure 6 where the maximum plasma electron distribution occurs approximately 4 ms after the pellet had entered the plasma, this being followed by a slow particle loss. Note: the electron confinement time for such plasmas is of the order of <10 ms [ref]. Finally, by comparing the net electron gain by the plasma after reproducible injections, with mean pellet particle content ($6.57\text{x}10^{18}$ +/-5% in Figure 6), a value of ~36% for fuelling efficiency is obtained for this example.

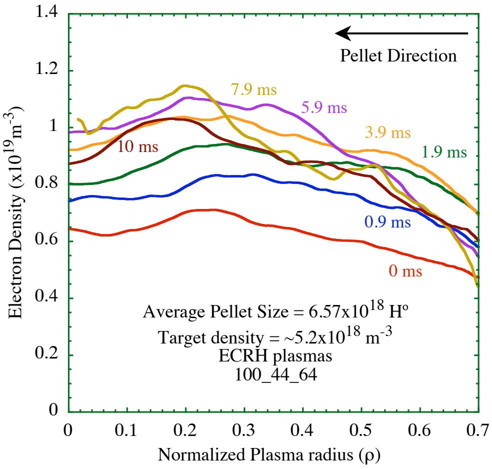

FIG. 5. Evolution of electron density profiles after pellet injection (pellet reaches plasma edge at 0 ms) for a series of reproducible ECRH discharges (#41779 to 41788).

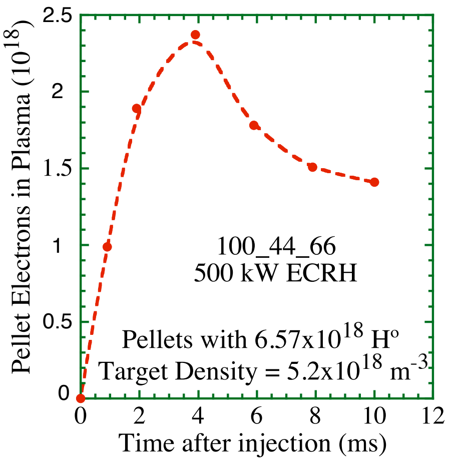

FIG. 6. Pellet electron population evolution in plasma after injection into reproducible ECRH plasmas (#41779 to 41788).

An example of multiple injections into NBI heated plasmas was presented in Figure 3. For such plasmas, the target electron temperature and density are significantly lower and higher, respectively, with respect to ECRH cases. In addition, larger pellets can typically be injected. In Figure 7, where a *Type*-2 pellet with $9.5\text{x}10^{18}$ H° was injected at 970 m/s, the electron temperature is seen to recover to its pre-injection values within a few milliseconds whilst the deposited pellet electrons undergo partial diffusion, and subsequent enhanced central confinement, arising from neoclassical

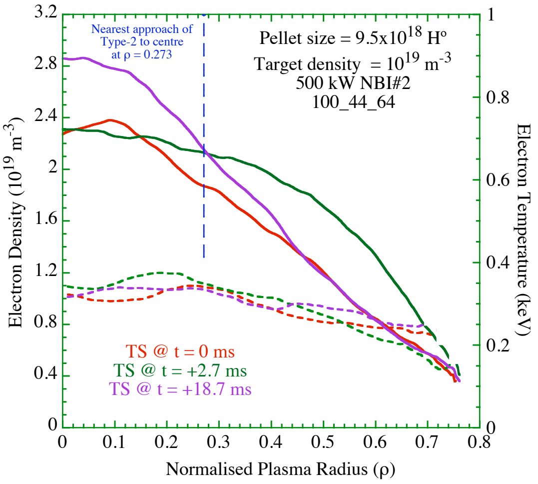

FIG. 7. Electron density and temperature profiles recorded before and after pellet injection into reproducible NBI heated plasmas.

transport [12]. Note: for Figure 7, the initial pellet fuelling efficiency is ~34%, with ~7% of pellet particles remaining in the plasma core 18.7 ms after injection. Additional injections, with *Type*-2 and with larger *Type*-3 pellets, into ECRH and NBI heated plasmas having a broad range of target densities are considered in Figure 8 as a function of target density. It is apparent from Figure 8 that fuelling efficiency in the TJ-II ends to improve with increasing target density (or with decreasing electron temperature), a finding that is consistent with that reported in reference [8]. It should be noted that several injections were made into plasmas created and maintained using NBI heating only. In such cases, the fuelling efficiency is significantly improved when compared to neighbouring points, this being explained by enhanced core pellet ablation due to impacts of suprathermal electrons that populate the core in such plasmas. The central location of suprathermal electrons is confirmed by an abrupt enhanced H_α ablation emission in the core. See for instance the H_α profile for discharge #37984 of Figure 2 in reference [11]. It should also be noted that the *Type*-3 pellet, injected into plasma with a central electron density of 4.2×10^{19} m^{-3}, has a reduced fuelling efficiency (~58%) when compared with the two *Type*-2 pellets injected under similar conditions. This is because this *Type*-3 pellet is not fully ablated in the plasma and part of it exits the plasma high-field side. Nonetheless, the observations described here require further analysis, in particular more data are needed to confirm, or confute, such tendencies.

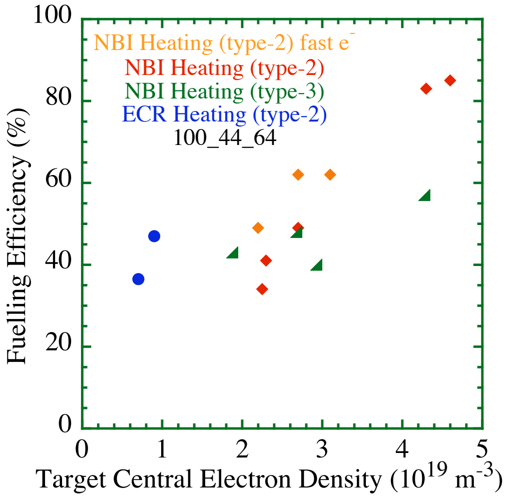

FIG. 8. Fuelling efficiencies for a range of target electron densities, heating modes and pellet types. Here "fast e^-" refers to plasmas created using NBI only - a significant plasma current remaining when an injection was made.

4. Discussion

Several pellet injections studies have been performed since the commissioning of the cryogenic pellet injector on the stellarator TJ-II. Here, a first study of fuelling by pellets in the core of this device is reported. It has revealed a tendency for improved fuelling efficiency with increased target density but with nuances that depend pellet size and experiment set-up. These will be studied in more detail in future experiments.

5. Acknowledgements

This work has been carried out within the framework of the EUROfusion Consortium and has received funding from the Euratom research and training programme 2014-2018 under grant agreement No 633053. The views and opinions expressed herein do not necessarily reflect those of the European Commission. In addition, it is partially financed by a grant from the Spanish Ministerio de Ciencia y Innovación (Ref. ENE2013-48679-R). The authors thank the TJ-II team for their assistance with the work.

References

[1] BAYLOR, L.R., PARKS, P.B., JERNIGAN, T.C., CAUGHMAN, J.B., COMBS, S.K., FOUST, C.R., HOULBERG, W.A., MARUYAMA, S., and RASMUSSEN, D.A. "Pellet fuelling and control of burning plasmas in ITER", Nucl. Fusion **47** (2007) 443.

[2] POLEVOI, A.R., SHIMADA, M., SUGIHARA, M., IGITKHANOV, YU L., MUKHOVATOV, V.S., KUKUSHKIN, A.S., MDEVEDEV, S.YU, ZVONKOV, A.V., and IVANOV, A.A., "Requirements for pellet injection in ITER scenarios with enhanced particle confinement", Nucl. Fusion **45** (2005) 1451.

[3] SPETH, E., "Neutral beam heating of fusion plasmas", Rep. Prog. Phys. **52** (1989) 57.

[4] BEIDLER, C.D., ALLMAIER, K., ISAEV, M.YU., KASILOV, S.V., KERBICHLER, W., LEITOLD, G.O., MAAßBERG, H., MIKKELSEN, D.R., MURAKAMI, S., SCHMIDT, M., SPRONG, D.A., TRIBALDOS, V., and WAKASA, A., "Benchmarking of the monoenergetic transport coefficients. Results from the international collaboration on neoclassical transport in stellarators (ICNTS)", Nucl. Fsuion **51** (2011) 076001.

[5] MAAßBERG, H., BEIDLER, C.D., and SIMMET, E.E., "Density control problems in large stellarators with neoclassical transport", Plasma Phys. Control. Fusion **41** (1999).

[6] MILORA, S.L., HOULBERG, W.A., LENGYEL L.L., and MERTENS, V., "Pellet fuelling", Nucl. Fusion **35** (1995).

[7] PÉGOURIÉ, B., "Pellet injection experiments and modelling", Plasma Phys. Control. Fusion **49** (2007) R87.

[8] BALDZUHN, J., BAYLOR, L.R., LYON, J.F, and W7-AS TEAM, "Penetration studies for deuterium pellets in Wendelstein 7-AS", Fusion Sci. Tech. **46** (2004) 348.

[9] YAMADA, H., SAKAMOTO, R., ODA, Y., HIRAMATSU, T., KINOSHITA, M., OGINO, M., MATSUDA, R., SUDO, S., KATO, S., FISHER, S.W., BAYLOR, L.R., and GOUGE, M., "Development of pellet injector system for large helical device", Fusion Eng. Des. **49-50** (2000) 915.

[10] SAKAMOTO, R., YAMADA, H., TAKEIRI, Y., NARIHARA, K., TOKOZUWA, T., SUZUKI, H., MASUZAKI, S., SAKAKIBARA, S., MORITA, S., GOTO, M., PETERSON, B.J., MATSUOKA, K., OHYABU, N., KOMORI, A. MOTOJIMA, O., and THE LHD EXPERIMENTAL GROUP, "Repetitive pellet fuelling for high-density/steady-state operation on LHD", Nucl. Fusion **46** (2006) 884.

[11] McCARTHY, K.J., PANADERO, N., ARAPOGLOU, I., COMBS, S.K., CAUGHMAN, J.B.O., de la CAL, E., FOUST, C., GARCÍA, R., HERNÁNDEZ SÁNCHEZ, J., MARTÍN, F., NAVARRO, M., PASTOR, I., RODRÍGUEZ, M.C., and VELASCO, J.L., "The pellet injector and its associated diagnostics for performing plasma studies on the TJ-II stellarator", 1st EPS Conference on Plasma Diagnostics, *Frascati*, *Italy*, Proc. of Science (ECPD2015) 134.

[12] VELASCO, J.L., McCARTHY, K.J., PANADERO, N., SATAKE, S., LÓPEZ-BRUNA, D., ALONSO, A., CALVO, I., DINKLAGE, A., ESTRADA, T., FONTDECABA, J.M., HÉRNANDEZ, J., GARCÍA, R., MEDINA, F., OCHANDO, M., PASTOR, I., PERFILOV, S., SÁNCHEZ, E., SOLETO, A., van MILLIGEN, B.PH., ZHEZERA, A., and THE TJ-II TEAM, "Transient particle transport after pellet injection in the TJ-II stellarator", Plasma Phys. Control. Fusion **58** (2016) 084004.

[13] McCARTHY, K.J., BALDZUHN, J., SAKAMOTO, R., DINKLAGE, A., CATS, S., MOTOJIMA, G., PANADERO, N., PÉGOURIÉ, B., YAMADA, H., ASCASÍBAR, E., THE LHD TEAM, THE W7-X TEAM and THE TJ-II TEAM, Proc. 20th Int. Stellarator/Heliotron Workshop (2015, Greifswald, Germany).

[14] SÁNCHEZ J., et al., "Dynamics of flows and confinement in the TJ-II stellarator", Nucl. Fusion **53** (2013) 104016.

[15] GUASP, J., and Liniers, M., "Loss cone structure for ions in the TJ-II helical axis stellarator. Part II: Radial electric field effects", Nucl. Fusion **40** (2000) 397.

[16] TABARÉS, F.L., OCHANDO, M., TAFALLA, D., MEDINA, F., McCARTHY, K., FONTDECABA, J.M., LINIERS, M., GUASP, J., ASCASÍBAR, E., ESTRADA, T., PASTOR, I., and the TJ-II TEAM, "Energy and particle balance studies under full boron and lithium-coated walls in TJ-II", Contrib. Plasma Phys. **50** (2010) 610.

[17] COMBS, S.K., FOUST, C.R., McGILL, J.M., CAUGHMAN, J.B.O., McCARTHY, K.J., BAYLOR, L.R., CHAMORRO, M., FEHLING, D.T., GARCIA, R., HARRIS, J.H., HERNÁNDEZ SÁNCHEZ, J., HIDALGO, C., MEITNER, S.J., RAMUSSEN, D.A. and UNAMUNO, R., "Results from laboratory testing of a new four-barrel pellet injector for the TJ-II stellarator", Fusion Sci. Tech. **64** (2013) 513.

[18] McCARTHY, K.J., *Diagnostic tools for probing hot magnetically confined plasmas*, XXXIII Reunión Bienal de la Real Sociedad Española de Física: 21er Encuentro Ibérico para la Enseñanza de la Física: PUBliCan, ediciones de la Universidad de Cantabria, Santander, Spain, **IV** (2011) 65. ISBN 978-84-86116-40-8

[19] HERRANZ, J., CASTEJÓN, F., PASTOR I., and McCARTHY, K.J., "The spectrometer of the high-resolution multiposition Thomson scattering diagnostic for TJ-II", Fusion Eng. Des. **65** (2003) 525.

[20] BAIÃO, D., MEDINA, F., OCHANDO, M., McCARTHY, K.J., TABARÉS, F., PASTOR, I., and VARANDAS, C., "Central electron temperature estimations of TJ-II neutral beam injection heated plasmas based on the soft x-ray multi-foil technique", Rev. Sci., Instrum. **83** (2012) 053501.